International Journal of Biochemistry and Cell Biology 106 (2019) 21–25

Contents lists available at ScienceDirect

International Journal of Biochemistry and Cell Biology

journal homepage: www.elsevier.com/locate/biocel

Organelles in Focus

Mitochondrial Nucleoids: Superresolution microscopy analysis

Petr Ježek*, Tomáš Špaček, Jan Tauber, Vojtěch Pavluch

Department of Mitochondrial Physiology, No.75, Institute of Physiology of the Czech Academy of Sciences, Prague, Czech Republic

ARTICLE INFO

Keywords:
mtDNA
Nucleoids
3D superresolution microscopy
TFAM

ABSTRACT

The mitochondrion owns an autonomous genome. Double-stranded circular mitochondrial DNA (mtDNA) is organized in complexes with a packing/stabilizing transcription factor TFAM, having multiple roles, and proteins of gene expression machinery in structures called *nucleoids*. From hundreds to thousands nucleoids exist distributed in the matrix of mitochondrial reticulum network. A single mtDNA molecule contained within the single nucleoid is a currently preferred but questioned model. Nevertheless, mtDNA replication should lead transiently to its doubling within a nucleoid. However, nucleoid division has not yet been documented in detail. A 3D superresolution microscopy is required to resolve nucleoid biology occurring in ~100 nm space, having an advantage over electron microscopy tomography in resolving the particular protein components. We discuss stochastic vs. stimulated emission depletion microscopy yielding wide vs. narrow nucleoid size distribution, respectively. Nucleoid clustering into spheroids fragmented from the continuous mitochondrial network, likewise possible nucleoid attachment to the inner membrane is reviewed.

1. Introduction

The mitochondrion is composed by the predominantly interconnected tubular network, having a complex double membrane structure (Plecitá-Hlavatá and Ježek, 2016). The central tubule part, *matrix*, has a complex topology of an „infinite octopus“, and is interrupted by the extremely invaginated inner mitochondrial membrane (IMM), forming cristae. Cristae are perpendicularly protruding nearly up to the opposite tubule side, but form a continuous membrane, the non-invaginated portion of which is termed the inner boundary membrane (IBM). IBM forms an inner cylinder inside the tubules of the outer mitochondrial membrane (OMM). Upon mitochondrial fission, fragmented spheroids of ~2 μm are made from a tubule of 10 μm length and the same surface (Fig. 1A–C).

The mitochondrion possesses an autonomous intron-free genome of its own genetic code, represented by the double-stranded (ds) circular mitochondrial (mt) DNA (mtDNA) (Gustafsson et al., 2016). In mammals ~16 kb mtDNA (16 569 bp in humans), representing 1–2% of the total cell DNA, encodes for 13 subunits of the respiratory chain complexes and ATP synthase (by 11 mRNAs), 12S and 16S rRNA and 22 tRNAs required for mtDNA gene expression. An endosymbiotic origin of mitochondrion gifted mtDNA its high-density packing in resulting nucleoprotein complexes termed *mitochondrial nucleoids*. Packing is higher than in nucleosomes for nuclear DNA. A transcription factor *A* mitochondrial (TFAM) is bending mtDNA and so is the major factor responsible for the high mtDNA density (Ngo et al., 2011). Nucleoids also contain other DNA maintenance proteins and recruited proteins of mtDNA gene expression machinery (Gustafsson et al., 2016). The major question to be solved is how do newly replicated nucleoids unpack and subsequently separate? Electron tomography and superresolution microscopy would be required to elucidate this.

Several hundreds or even thousands of nucleoids exist within the mt network (Brown et al., 2011; Garrido et al., 2003; Tauber et al., 2013; Dlasková et al., 2015)(Fig. 1C), reflecting the fact that mtDNA is present in a cell in a high number of copies, termed the *copy number*. Existence of a single mtDNA molecule within the single nucleoid has been suggested based on the estimated average of 1.4 mtDNA per nucleoid in human fibroblasts (Kukat et al., 2011, 2015). However, this contradicts the average of 3 mtDNA molecules per nucleoid estimated for mouse embryonic fibroblast 3T3sw cells (Brown et al., 2011) and to a very

Abbreviations: ATAD3B, AAA-domain-containing protein 3 isoform B; dSTORM, direct stochastic optical reconstruction microscopy; FIB-SEM, focused ion beam ablation scanning electron microscopy; IBM, inner boundary membrane; IMM, inner mitochondrial membrane; LONP1, AAA protease La domain (Lon) peptidase 1; MRPL12, mitochondrial ribosomal protein L12; mt, mitochondrial; MTERF, mitochondrial transcription termination factor; mtSSB, mitochondrial single-stranded DNA binding protein; OMM, outer mitochondrial membrane; PALM, photoactivated localization microscopy; Pol-β, DNA polymerase β; Polγ, DNA polymeraseγ; POLRMT, RNA polymerase mitochondrial; STED, stimulated emission depletion (microscopy); TEFM, transcription elongation factor mitochondrial; TFAM, transcription factor A mitochondrial; TFB2M, transcription factor B2 mitochondrial

* Corresponding author at: Dept. No.75, Institute of Physiology of the Czech Academy of Sciences, Vídeňská 1083, 14220 Prague 4, Czech Republic.
E-mail address: jezek@biomed.cas.cz (P. Ježek).

https://doi.org/10.1016/j.biocel.2018.10.012
Received 18 July 2018; Received in revised form 11 October 2018; Accepted 15 October 2018
Available online 02 November 2018
1357-2725/

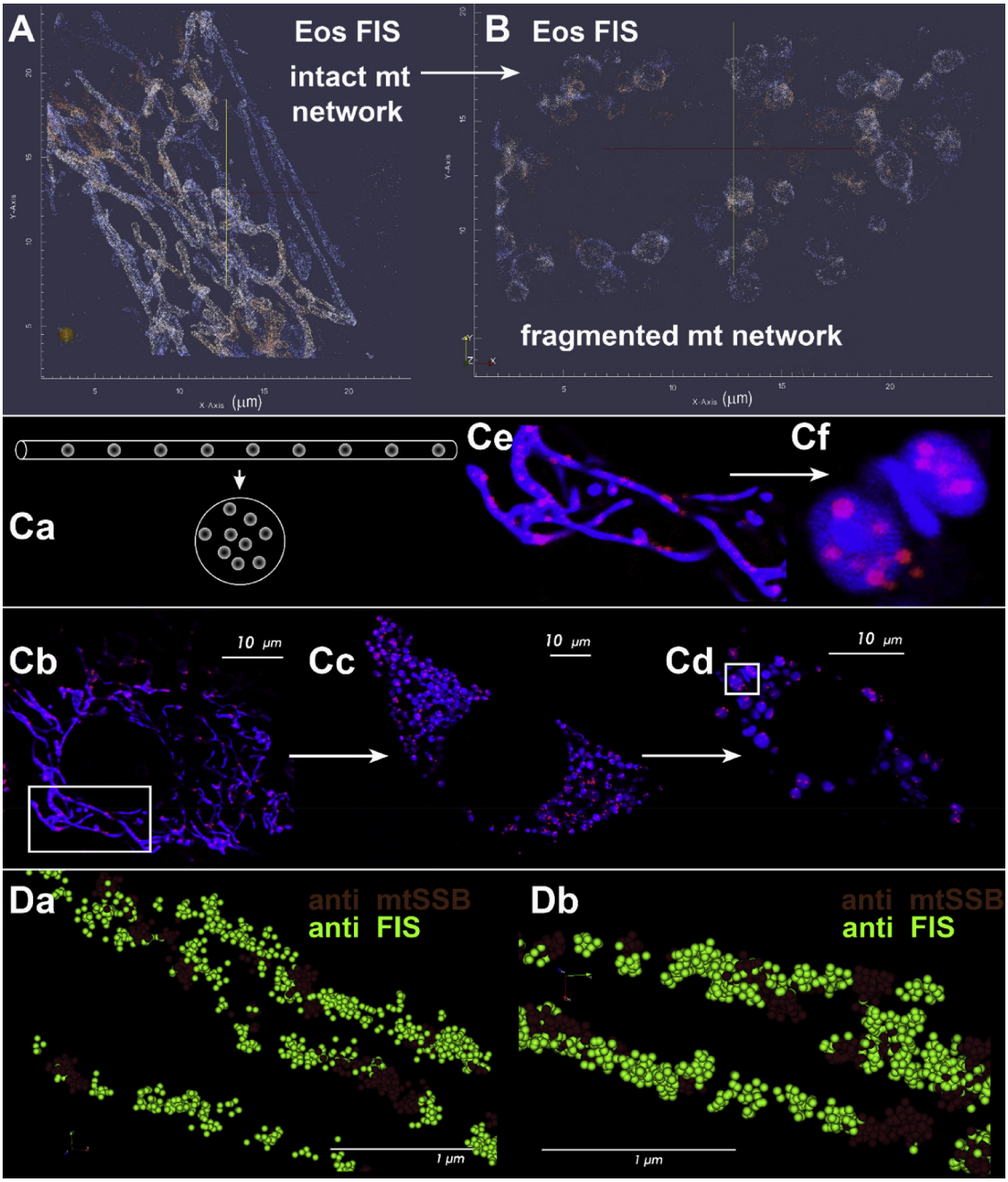

Fig. 1. Nucleoids inside the mitochondrial network tubules and their clustering upon fission.
A–C) Superresolution 3D FPALM imaging of intact (A) and fragmented mt network (B) in HepG2 cells, using FIS1-Eos2 conjugate overexpression as compared with overlays of conventional confocal microscopy 2D images (Cb–Cf), such as previously shown an interpreted as shown in scheme Ca (Tauber et al., 2013), for mtGFP-transfected cells (blue) and Alexa-568 immunostaining for mtSSB (magenta). Fragmentation was always induced by up to 0.1 μm valinomycin.
Note, such fragmentation is essential for the predicted selective mitochondrial-specific autophagy (mitophagy), where mt network fragments with low membrane potential are preferentially brought to lysosomes for degradation (Twig et al., 2008). Since low potential frequently originates from mutant or oxidized mtDNA within the particular fragment, mutant mtDNA is selectively eliminated in this process. Such process is a part of the clone expansion following the bootleneck effect during primordial oocyte formation (Cree et al., 2008).
D) 3D dSTORM superresolution imaging of mtSSB (brown) and OMM FIS1 (green) is shown for comparison at two selected images Da, Db. The centers of 50 nm spheres show positions of each localized fluorophore (antibody) during experiment. Sphere diameters demonstrate the uncertainty of their localization. Imaging performed as described by Alán et al. (2016).

similar number and large nucleoid size revealed in pancreatic β-cells of diabetic Goto Kakizaki rats, containing > 3 times less mtDNA than nondiabetic rats (Špaček et al., 2017). Consequently, the TFAM:mtDNA stoichiometry should vary. Also, human TFAM overexpression in mouse fibroblasts, yielding 2.5 higher TFAM content, did not increase nucleoid size, but only induced a twice as high nucleoid number (Kukat et al., 2015).

Replication of mtDNA must lead transiently to two mtDNA molecules per nucleoid. After mtDNA replication within a single nucleoid, a state must follow, when nucleoid division takes place. Hypothetically, unpacked nucleoids upon replication subsequently separate following termination of replication. Theoretically, two new nucleoids should

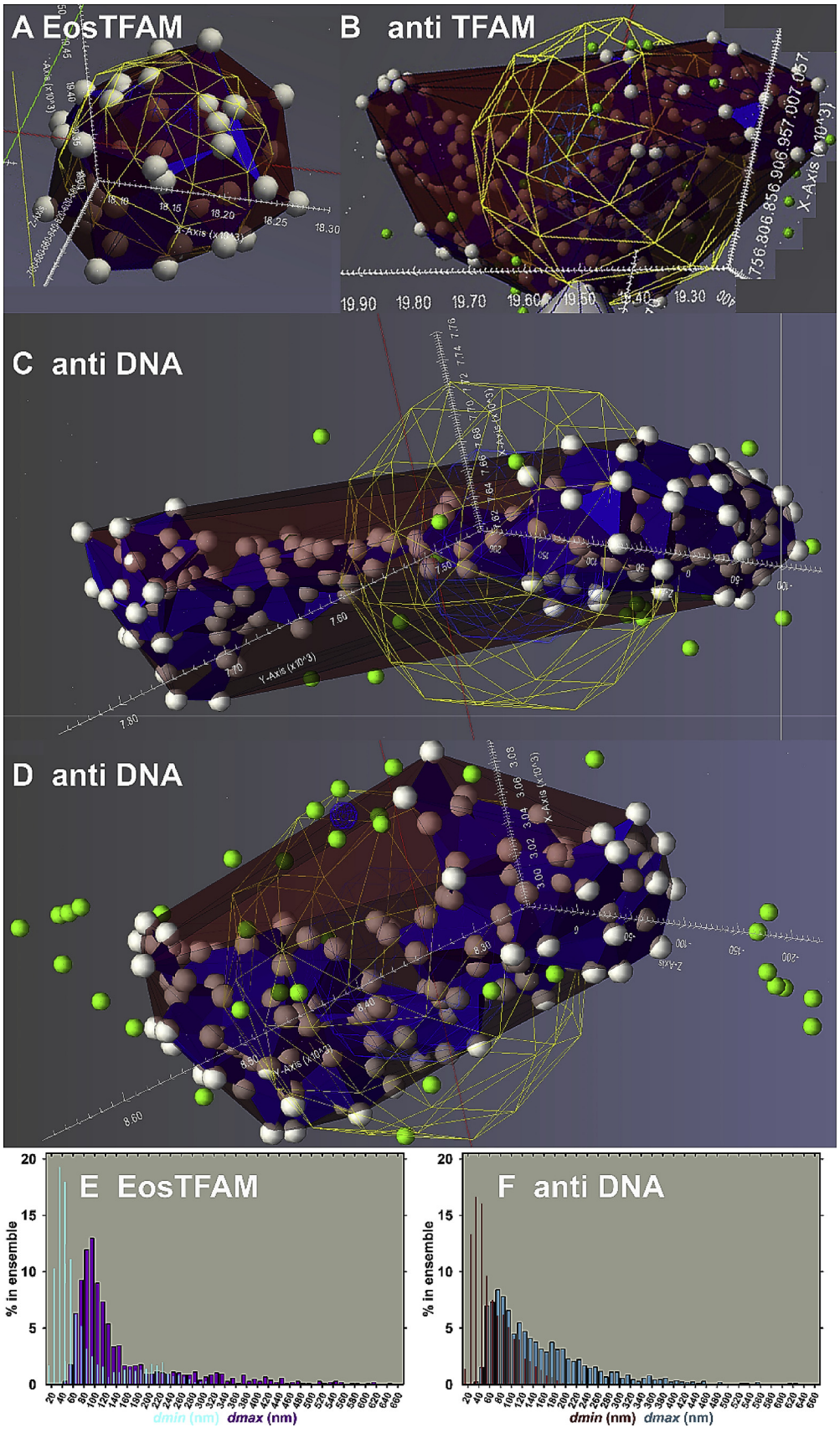

Fig. 2. Nucleoid topology and size distribution.

A–D) Topology of a typical nucleoid (A) and nucleoid twins probably originating from nucleoid division (B–D): nucleoid models of HepG2 cells are shown such as described by Alán et al. (2016) for super-resolution 3D PALM microscopy using TFAM-Eos2 conjugate overexpression (A) and 3D dSTORM using antiTFAM (B) and antiDNA antibodies (C, D). White 25 nm spheres demonstrate uncertainty of localization (superresolution), while blue polyhedrons of 80 nm base resulted from Delaunay segmentation/tessellation, and red translucent sphapes show its maximum space. Yellow spheres are drawn having the same volume as Delaunay polyhedrons. Green points were excluded during segmentation.

E,F) Histograms of the long and short sizes of rotational ellipsoid models for HepG2 cell nucleoids. Data of Alán et al. (2016) for several cells and using 3D PALM microscopy with TFAM-Eos2 (E) and 3D dSTORM using antiDNA antibodies (F) provide the similar most frequent ellipsoid long sizes as reported for STED by Kukat et al. (2011), but demonstrate a wide range of nucleoid size.

result from replication after certain steps. However, nucleoid division has not yet been distinguished from nucleoid collisions (Fig. 2A–D).

The mtDNA packing is ensured by TFAM, which coats whole mtDNA at a stoichiometry ~900:1 (450 binding sites on ds ~16 kb mtDNA) in human mitochondrion (Alam et al., 2003). Compaction of mtDNA requires a cross-strand TFAM binding with footprints of 10–30 bp, as deduced from in vitro reconstitutions (Kukat et al., 2015). TFAM forms a U-turn on mtDNA by inserting the highly mobile domains (HMG-box) A and B into small grooves at a half sites of the mtDNA duplex. A positively charged spiral coupler between these domains interacts with the negatively charged mtDNA (Ngo et al., 2011). TFAM dimerization was first suggested (Ngo et al., 2011), but later excluded to be essential for complete mtDNA compaction. TFAM bound to mtDNA can form oligomers compacting mtDNA to even higher density (Kukat et al., 2015). The mitochondrial AAA proteases Lon peptidase-1 (LONP1) degrades preferentially free TFAM and thus regulates the TFAM:mtDNA stoichiometry (Lan et al., 2017). PKA- or ERK-mediated phosphorylation of TFAM prevents TFAM binding to mtDNA and thus renders LONP1 to TFAM degradation (Lu et al., 2013). In conclusion, TFAM is not only a nucleoid structural protein due to sequence-nonspecific binding, but also a transcription factor, promoter selector, and replication initiator (by sequence-specific binding) and the regulator of the mtDNA copy number (Kang et al., 2018).

2. Nucleoid function

In general, nucleoids allow mtDNA to be dispersed and segregated in numerous loci within the mt network. The three major events, mtDNA replication, mtDNA transcription and repair of mtDNA, then belong to the major functions of nucleoids (Gustafsson et al., 2016; Kang et al., 2018). The mtDNA replication is constantly repeated within the so-called D-loop, beyond which proceeds after proper regulatory stimuli (Gustafsson et al., 2016). Transcription of mtDNA intercepts mtDNA replication. Nucleoids should at least partly open their structures at the different stages of replication or transcription.

The mtDNA replication is substantiated by the DNA polymerase γ (Pol-γ) (Gustafsson et al., 2016; Rajala et al., 2014), with essential help by the TWINKLE helicase, unwinding mtDNA (Milenkovic et al., 2013), in concert with TFAM and the tetrameric mt single-stranded DNA binding protein (mtSSB, Fig. 1D) (Ruhanen et al., 2010) and mt topoisomerases; but also mtRNA polymerase (POLRMT), making primers, plus RNase H1, degrading primers; and RNase MRP, essential for the L-strand initiation. Duration of mtDNA replication is about 1 h with a presumed single nucleoid division in each 40 s (Sasaki et al., 2017).

The mtDNA transcription, resulting in large polycistrons from both strands, is performed by a single-subunit, factor dependent, RNA polymerase POLRMT, recruited by TFAM. The N-terminus of POLRMT binds to TFAM at an open mtDNA upon further recruitment of the mt transcription factor B2 (TFB2M) to achieve a promoter-specific initiation (Gustafsson et al., 2016; Hillen et al., 2017). The mt transcription elongation factor (TEFM), transcription termination factor (MTERF), and mt ribosomal protein L12 (MRPL12) are required (Rorbach and Minczuk, 2012). Nucleoids should unwind mtDNA in the transcribing loci, but until a certain moment the resulting polycistronic RNA can be still attached. Consequently, when stained for RNA or transcription proteins (including TFAM), nucleoids may appear larger.

The mutation rate for mtDNA vs. nuclear DNA was estimated to be 10–17-fold higher. Since mtDNA is vulnerable to oxidative stress and oxidized nucleotide bases are transformed into mtDNA mutations, repair mechanisms exist, similarly as for nuclear DNA, and act within the nucleoid structures. DNA polymerase β (Pol-β) ensures repair of oxidized/mutated mtDNA (Sykora et al., 2017).

Also, nucleoid connections to IMM are plausible (Brown et al., 2011; Kopek et al., 2012), since the rich cristae comb (enfolded IMM) is ubiquitous within mt tubules (Kukat et al., 2015; Kopek et al., 2012). A single nucleoid should fit into a space, where several cristae are missing, and there is a high probability to encounter IMM. TFAM-labeled nucleoids were found to be located either as adjacent to the intracristal space (visualized by Dronpa-lactamase β) or even surrounded by the intracristal space (Brown et al., 2011; Kopek et al., 2012; Kukat et al., 2015). Protein complexes joining nucleoid proteins with IMM proteins have yet to be carefully verified. Certain nucleoid-IMM connecting proteins are expressed only in stem cells or cancer cells, such as the ATPase family AAA-domain-containing protein 3 isoform B (ATAD3B), connecting the non-coding D loop of mtDNA with the IMM (Baudier, 2018).

Nucleoids are typically surrounded and maybe spatially coordinated with so-called RNA granules, i.e. complexes of RNase P with newly synthesized mtRNA, containing an RNA-binding protein G-rich sequence factor 1 GRSF1 (Antonicka et al., 2013). Also mt ribosomes are found in nucleoid proximity, while colocalization is ensured for OMM-attached nuclear ribosomes, protein import complexes and mt ribosomes to assist IMM assembly for respiratory chain complexes or ATP-synthase (Gustafsson et al., 2016).

3. Cell physiology of mitochondrial nucleoids

Cell physiology of nucleoids is still rather unknown and might be ideally studied by the emerging time-resolved superresolution fluorescence microscopy (Dlasková et al., 2018; Sahl et al., 2017). Applied 2D superresolution, but purely physical, technique, the stimulated emission depletion (STED) microscopy, Kukat et al. (2011) reported only a narrow range of nucleoid sizes around 100 nm. In contrast, 3D imaging in a 4Pi mode of photoactivated localization microscopy (iPALM) using a monomeric Eos2-conjugate of TFAM showed a very wide range of nucleoid sizes from 31 to 318 nm (Brown et al., 2011; Kopek et al., 2012). The iPALM 4D superresolution fluorescence microscopy technique was also combined with the focused ion beam ablation scanning electron microscopy (FIB-SEM) (Kopek et al., 2012). This combination allowed projections of nucleoid structures contoured by TFAM into the mitochondrial tubule sections with emphasized cristae. Images revealed nucleoids in sections with dimensions of ~100 nm intercepting parallel cristae, but also cristae-free regions with apparent nucleoid clusters spanning a 350 nm area. Even such a high 3D resolution (20 nm in the xy-plane) did not distinguish whether there are larger single nucleoids or dense clusters of smaller ~100 nm nucleoids. None of the large clusters was homogeneously covered by TFAM.

The resulting 3D maps of TFAM-visualized nucleoids together with cristae membranes clearly indicated that the assumed ellipsoidal nucleoid shape is a rough idealization. Instead, protrusions exist of TFAM-contained nucleoid “fingers” between cristae tips and e.g. only a portion of a 350 nm “nucleoid” (or cluster) was found compact, when residing in the adjacent cristae free matrix space – cf. figure 3 in (Kopek et al., 2012). Unlike nucleoids imaged by STED, the iPALM TFAM-contoured 3D images of nucleoids exhibited a variety of sizes and shapes. Even amorphous or branched nucleoids were found (Brown et al., 2011). The latter might represent active or dividing nucleoids (Fig. 2B–D).

A similar wide nucleoid size distribution has always been observed when stochastic 3D superresolution microscopy was employed (Alán et al., 2016; Brown et al., 2011; Dlasková et al., 2018; Špaček et al., 2017) (Fig. 2E), as well as when mtDNA was visualized by the 3D direct stochastic optical reconstruction microscopy (dSTORM), a superresolution variant of 3D immunocytochemistry (Alán et al., 2016; Brown et al., 2011; Dlasková et al., 2018; Špaček et al., 2017) (Fig. 2F). Localized points were modeled into nucleoid 3D images either using the probability density values (Brown et al., 2011) or Delaunay segmentation (Alán et al., 2016; Dlasková et al., 2018; Špaček et al., 2017) (Fig. 2 A–D) or nucleoid dimensions could be roughly derived from the Ripley’s K-function (Dlasková et al., 2018). One cannot judge which morphology in the obtained superresolution images of nucleoids reflects the true native state, unless the pure physical (such as STED) and

stochastic 3D imaging is performed on the same sample.

The Delaunay segmentation identified nucleoid twins, which were hypothetically assigned to nucleoids immediately after the nucleoid division (Alán et al., 2016) (Fig. 2B–D). Twins had already been observed previously (Brown et al., 2011). Despite the low resolution, proximal nucleoids were also found by conventional confocal microscopy (Garrido et al., 2003). In living cells, nucleoids were observed to be constantly attached/detached from each other while remaining as discrete entities (Sasaki et al., 2017). In conclusion, nucleoid division has yet to be demonstrated as originating from the initial single mtDNA.

4. Pathology related to mitochondrial nucleoids

Mutations in mtDNA cause a plethora of human diseases (Lagouge and Larsson, 2013); likewise the pathology of numerous diseases including neurodegeneration is also induced by the impaired mitochondrial biogenesis including the causes of impaired TFAM function (Kang et al., 2018).

5. Future outlook

Molecular nucleoid physiology should be uncovered in the future, determining details of nucleoid division and relate it to the cell cycle and de novo biogenesis of mt network tubules; definitively establish number of mtDNA per nucleoid in different conditions, nucleoid attachment to the IMM, coordination of mtDNA replication; and vice versa, reveal clustering of nucleoids in mt fragments upon fission and conditions when are subjected to mitophagy. Without reaching this fundamental knowledge, pathology related to mtDNA maintenance defects cannot be elucidated.

Acknowledgements

Dr. P.J was supported by grants awarded by the Grant Agency of the Czech Republic No. 16-04788S and 17-01813S.

References

Alam, T.I., Kanki, T., Muta, T., Ukaji, K., Abe, Y., Nakayama, H., Takio, K., Hamasaki, N., Kang, D., 2003. Human mitochondrial DNA is packaged with TFAM. Nucleic Acids Res. 31, 1640–1645.

Alán, L., Špaček, T., Ježek, P., 2016. Delaunay algorithm and principal component analysis for 3D visualization of mitochondrial DNA nucleoids by Biplane FPALM/dSTORM. Eur. Biophys. J. 45, 443–461. https://doi.org/10.1007/s00249-016-1114-5.

Antonicka, H., Sasarman, F., Nishimura, T., Paupe, V., Shoubridge, E.A., 2013. The mitochondrial RNA-binding protein GRSF1 localizes to RNA granules and is required for posttranscriptional mitochondrial gene expression. Cell Metab. 17, 386–398. https://doi.org/10.1016/j.cmet.2013.02.006.

Baudier, J., 2018. ATAD3 proteins: brokers of a mitochondria-endoplasmic reticulum connection in mammalian cells. Biol. Rev. Camb. Philos. Soc. 93, 827–844. https://doi.org/10.1111/brv.12373.

Brown, T.A., Tkachuk, A.N., Shtengel, G., Kopek, B.G., Bogenhagen, D.F., Hess, H.F., Clayton, D.A., 2011. Superresolution fluorescence imaging of mitochondrial nucleoids reveals their spatial range, limits, and membrane interaction. Mol. Cell. Biol. 31, 4994–5010. https://doi.org/10.1128/MCB.05694-11.

Cree, L.M., Samuels, D.C., de Sousa Lopes, S.C., Rajasimha, H.K., Wonnapinij, P., Mann, J.R., Dahl, H.H., Chinnery, P.F., 2008. A reduction of mitochondrial DNA molecules during embryogenesis explains the rapid segregation of genotypes. Nat. Genet. 40, 249–254. https://doi.org/10.1038/ng.2007.63.

Dlasková, A., Engstová, H., Plecitá-Hlavatá, L., Lessard, M., Alán, L., Reguera, D.P., Jabůrek, M., Ježek, P., 2015. Distribution of mitochondrial DNA nucleoids inside the linear tubules vs. Bulk parts of mitochondrial network as visualized by 4Pi microscopy. J. Bioenerg. Biomembr. 47, 255–263. https://doi.org/10.1007/s10863-015-9610-3.

Dlasková, A., Engstová, H., Špaček, T., Kahancová, A., Pavluch, V., Smolková, K., Špačková, J., Bartoš, M., Hlavatá, L.P., Ježek, P., 2018. 3D super-resolution microscopy reflects mitochondrial cristae alternations and mtDNA nucleoid size and distribution. Biochim. Biophys. Acta 1859, 829–844. https://doi.org/10.1016/j.bbabio.2018.04.013.

Garrido, N., Griparic, L., Jokitalo, E., Wartiovaara, J., van der Bliek, A.M., Spelbrink, J.N., 2003. Composition and dynamics of human mitochondrial nucleoids. Mol. Biol. Cell 14, 1583–1596. https://doi.org/10.1091/mbc.e02-07-0399.

Gustafsson, C.M., Falkenberg, M., Larsson, N.-G., 2016. Maintenance and expression of mammalian mitochondrial DNA. Annu. Rev. Biochem. 85, 133–160. https://doi.org/10.1146/annurev-biochem-060815-014402.

Hillen, H.S., Morozov, Y.I., Sarfallah, A., Temiakov, D., Cramer, P., 2017. Structural basis of mitochondrial transcription initiation. Cell 171, 1072–1081. https://doi.org/10.1016/j.cell.2017.10.036. e10.

Kang, I., Chu, C.T., Kaufman, B.A., 2018. The mitochondrial transcription factor TFAM in neurodegeneration: emerging evidence and mechanisms. FEBS Lett. 592, 793–811. https://doi.org/10.1002/1873-3468.12989.

Kopek, B.G., Shtengel, G., Xu, C.S., Clayton, D.A., Hess, H.F., 2012. Correlative 3D superresolution fluorescence and electron microscopy reveal the relationship of mitochondrial nucleoids to membranes. Proc. Natl. Acad. Sci. U.S.A. 109, 6136–6141. https://doi.org/10.1073/pnas.1121558109.

Kukat, C., Wurm, C.A., Spåhr, H., Falkenberg, M., Larsson, N.-G., Jakobs, S., 2011. Super-resolution microscopy reveals that mammalian mitochondrial nucleoids have a uniform size and frequently contain a single copy of mtDNA. Proc. Natl. Acad. Sci. U.S.A. 108, 13534–13539. https://doi.org/10.1073/pnas.1109263108.

Kukat, C., Davies, K.M., Wurm, C.A., Spåhr, H., Bonekamp, N.A., Kühl, I., Joos, F., Polosa, P.L., Park, C.B., Posse, V., Falkenberg, M., Jakobs, S., Kühlbrandt, W., Larsson, N.G., 2015. Cross-strand binding of TFAM to a single mtDNA molecule forms the mitochondrial nucleoid. Proc. Natl. Acad. Sci. U.S.A. 112, 11288–11293. https://doi.org/10.1073/pnas.1512131112.

Lagouge, M., Larsson, N.G., 2013. The role of mitochondrial DNA mutations and free radicals in disease and ageing. J. Intern. Med. 273, 529–543. https://doi.org/10.1111/joim.12055.

Lan, L., Guo, M., Ai, Y., Chen, F., Zhang, Y., Xia, L., Huang, D., Niu, L., Zheng, Y., Suzuki, C.K., Zhang, Y., Liu, Y., Lu, B., 2017. Tetramethylpyrazine blocks TFAM degradation and up-regulates mitochondrial DNA copy number by interacting with TFAM. Biosci. Rep. 37 (3). https://doi.org/10.1042/BSR20170319.

Lu, B., Lee, J., Nie, X., Li, M., Morozov, Y.I., Venkatesh, S., Bogenhagen, D.F., Temiakov, D., Suzuki, C.K., 2013. Phosphorylation of human TFAM in mitochondria impairs DNA binding and promotes degradation by the AAA+ Lon protease. Mol. Cell 49, 121–132. https://doi.org/10.1016/j.molcel.2012.10.023.

Milenkovic, D., Matic, S., Kühl, I., Ruzzenente, B., Freyer, C., Jemt, E., Park, C.B., Falkenberg, M., Larsson, N.G., 2013. TWINKLE is an essential mitochondrial helicase required for synthesis of nascent D-loop strands and complete mtDNA replication. Hum. Mol. Genet. 22, 1983–1993. https://doi.org/10.1093/hmg/ddt051.

Ngo, H.B., Kaiser, J.T., Chan, D.C., 2011. The mitochondrial transcription and packaging factor Tfam imposes a U-turn on mitochondrial DNA. Nat. Struct. Mol. Biol. 18 (2011), 1290–1296. https://doi.org/10.1038/nsmb.2159.

Plecitá-Hlavatá, L., Ježek, P., 2016. Integration of superoxide formation and cristae morphology for mitochondrial redox signaling. Int. J. Biochem. Cell Biol. 80, 31–50. https://doi.org/10.1016/j.biocel.2016.09.010.

Rajala, N., Gerhold, J.M., Martinsson, P., Klymov, A., Spelbrink, J.N., 2014. Replication factors transiently associate with mtDNA at the mitochondrial inner membrane to facilitate replication. Nucleic Acids Res. 42, 952–967. https://doi.org/10.1093/nar/gkt988.

Rorbach, J., Minczuk, M., 2012. The post-transcriptional life of mammalian mitochondrial RNA. Biochem. J. 444, 357–373. https://doi.org/10.1042/BJ20112208.

Ruhanen, H., Borrie, S., Szabadkai, G., Tyynismaa, H., Jones, A.W., Kang, D., Taanman, J.W., Yasukawa, T., 2010. Mitochondrial single-stranded DNA binding protein is required for maintenance of mitochondrial DNA and 7S DNA but is not required for mitochondrial nucleoid organization. Biochim. Biophys. Acta 1803, 931–939. https://doi.org/10.1016/j.bbamcr.2010.04.008.

Sahl, S.J., Hell, S.W., Jakobs, S., 2017. Fluorescence nanoscopy in cell biology. Nat. Rev. Mol. Cell Biol. 18, 685–701. https://doi.org/10.1038/nrm.2017.71.

Sasaki, T., Sato, Y., Higashiyama, T., Sasaki, N., 2017. Live imaging reveals the dynamics and regulation of mitochondrial nucleoids during the cell cycle in Fucci2-HeLa cells. Sci. Rep. 7, 11257. https://doi.org/10.1038/s41598-017-10843-8.

Špaček, T., Pavluch, V., Alán, L., Capková, N., Engstová, H., Dlasková, A., Berková, Z., Saudek, F., Ježek, P., 2017. Nkx6.1 decline accompanies mitochondrial DNA reduction but subtle nucleoid size decrease in pancreatic islet β-cells of diabetic Goto Kakizaki rats. Sci. Rep. 7, 15674. https://doi.org/10.1038/s41598-017-15958-6.

Sykora, P., Kanno, S., Akbari, M., Kulikowicz, T., Baptiste, B.A., Leandro, G.S., Lu, H., Tian, J., May, A., Becker, K.A., Croteau, D.L., Wilson 3rd, D.M., Sobol, R.W., Yasui, A., Bohr, V.A., 2017. DNA polymerase beta participates in mitochondrial DNA repair. Mol. Cell. Biol. https://doi.org/10.1128/MCB.00237-17. pii: MCB.00237-17.

Tauber, J., Dlasková, A., Šantorová, J., Smolková, K., Alán, L., Špaček, T., Plecitá-Hlavatá, L., Jabůrek, M., Ježek, P., 2013. Distribution of mitochondrial nucleoids upon mitochondrial network fragmentation and network reintegration in HEPG2 cells. Int. J. Biochem. Cell Biol. 45, 593–603. https://doi.org/10.1016/j.biocel.2012.11.019.

Twig, G., Elorza, A., Molina, A.J., Mohamed, H., Wikstrom, J.D., Walzer, G., Stiles, L., Haigh, S.E., Katz, S., Las, G., Alroy, J., Wu, M., Py, B.F., Yuan, J., Deeney, J.T., Corkey, B.E., Shirihai, O.S., 2008. Fission and selective fusion govern mitochondrial segregation and elimination by autophagy. EMBO J. 27, 433–446. https://doi.org/10.1038/sj.emboj.7601963.